

SNS Accumulator Ring Collimator Optimization with Beam Dynamics

SNS/ORNL/AP TECH NOTE

Number 010

D. Jeon, V.V. Danilov, J.D. Galambos, J.A. Holmes, D.K. Olsen

December 1998

SNS Accumulator Ring Collimator Optimization with Beam Dynamics

1. Introduction

Spallation Neutron Source (SNS) is the most powerful pulsed neutron source under construction with repetition rate of 60 Hz that accelerates proton beam up to 1 GeV with 1 MW initial beam power that is to be upgraded up to 4 MW. SNS operation requires acceleration of intense beam for which space charge effects may play an appreciable role. It is understood that a certain level of beam loss is unavoidable during operation of accumulator ring that comes from various sources such as halo generation due to space charge force, nonlinearities, errors and harmonic modulations etc. Hands-on maintenance requires that uncontrolled beam loss should be less than 1 nA/m at 1 GeV energy, which corresponds to 10^{-6} of 1 MW beam power per meter. Special collimators are in need which can absorb halo particles and contain activation due to secondary particles in order to meet the beam loss requirement. Figure 1 shows the straight section in the ring reserved for collimation. This straight section is shown with four collimators.

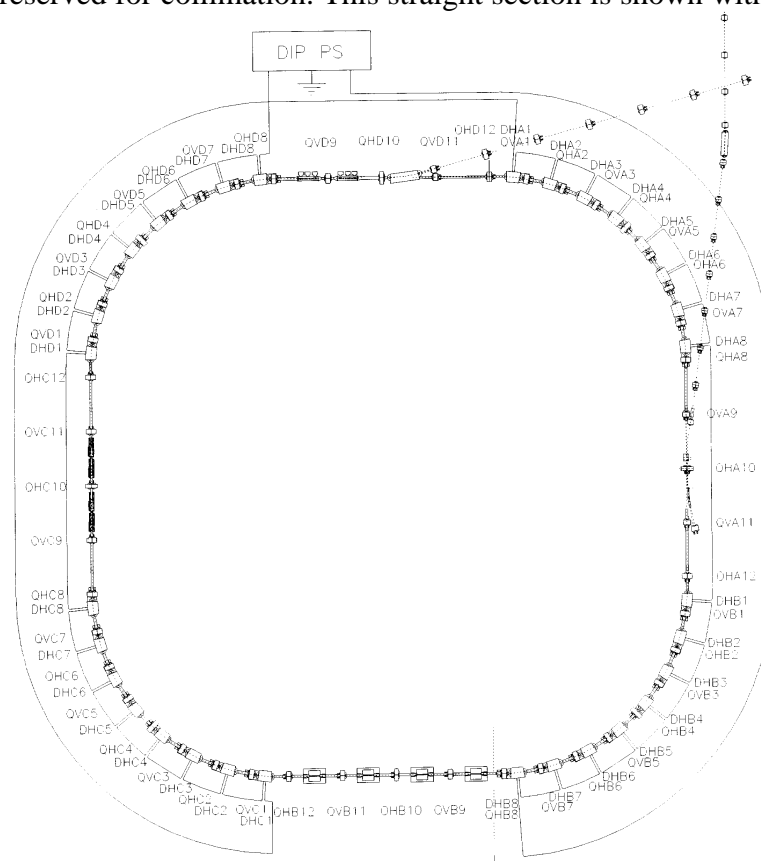


Fig. 1 Four collimators are located at the bottom straight section. Beam is circulating clockwise.

H. Ludewig of BNL designed a collimator using the LAHET code that absorbs halo particles and contains activation effectively. However, there still remain a few questions that need to be answered with beam dynamics. These questions are as follows:

- optimal length of inner collimating tube of collimators
- number and location of collimators
- aperture size of secondary collimators with respect to that of primary collimators to minimize activation of down stream beam line components
- on what components and at what level of activation are expected down stream from the collimators
- material of inner collimating tube
- how much residual halo is anticipated from the collimators?

2. Halo particle distribution

Numerical simulations are needed to obtain a reasonable halo particle distribution necessary for optimization of collimators. Even though the HEBT (High Energy Beam Transport) may be optically matched to the Accumulator Ring, there still could be some mismatch originating from that the distributions of injected particles may not be equilibrium distributions for the Accumulator Ring due to space charge effects. Simulations of injection and accumulation for 1158 turns were done for the nominal case where bare tunes are $n_x = 5.82$ and $n_y = 5.80$ by using the ACCSIM code with PIC (Particle-In-Cell) space charge routine. The ACCSIM code utilizes linear transfer matrix. The beam power at the final turn is set to 2 MW. These are realistic simulations of injection to accumulator ring with space charge effects. It is observed that a relaxation process in particle distribution takes place due to initial mismatch in particle distributions, and this mismatch drives halo formation. Of course, there are many mechanisms that induce particle diffusion such as nonlinearities, various kinds of errors including harmonic modulations, foil scattering, residual gas scattering etc. So we need to make a conservative estimation on the halo particle diffusion rate.

Figure 2 shows emittance (loosely defined to be $2pJ$) plots of halo particles versus turn number whose x or y emittance is larger than $180 p$ mm mrad where the collimators are placed. It is important to note that the halo particles with large x (y) emittance correspond to those with small y (x) emittance. In the simulation, 100 macro particles are injected every turn for 1158 turns with 2 MW final beam power. Halo above $180 p$ mm mrad starts to appear after 800 turns in y phase space. The reason why halo generation favors y phase space is partly due to dispersion in x (horizontal) which alleviates space charge effects and partly due to slightly stronger focusing in x (x bare tune without space charge effects is 5.82 while y bare tune is 5.80). Figure 2 shows that the diffusion rate is about 0.25 (0.19) p mm mrad/turn in y (x) phase space. It is worth pointing out that the diffusion in stochastic region which causes the halo formation depicted in Fig. 2 is bounded by stable tori even though it is not clear in this figure. The extent of the

stochastic region and position of these stable tori depend on the strength of the driving force that is a function of mismatch.

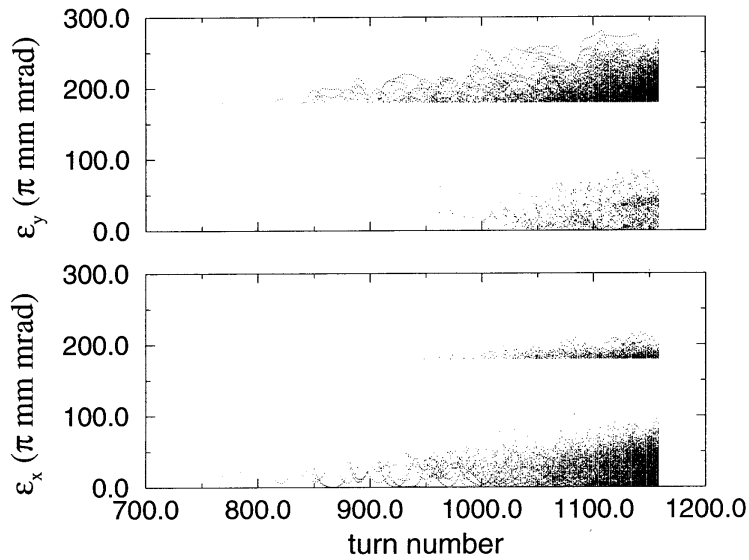


Fig. 2 Emittance plots of halo particles versus turn number whose x or y emittance is larger than $180 \mu\text{m mrad}$. There are two groups of particles in both plots. The bottom group in top (bottom) plot represents y (x) emittance of halo particles whose x (y) emittance is larger than $180 \mu\text{m mrad}$.

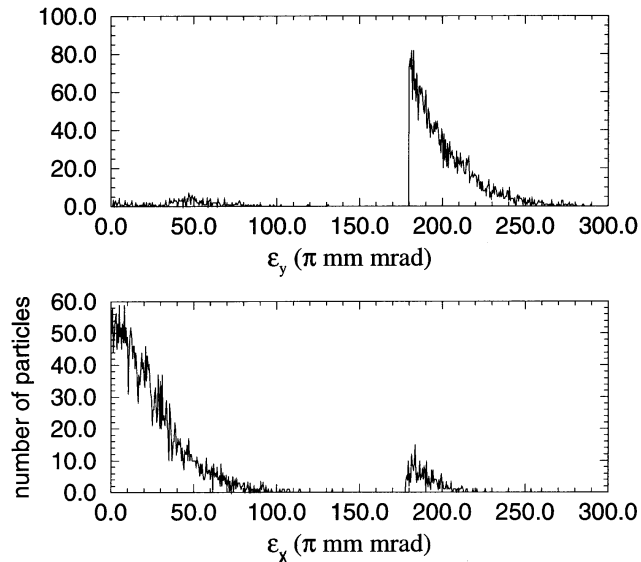


Fig. 3 Plots of emittance of halo particles obtained from numerical simulation are shown whose x or y emittance is larger than $180 \mu\text{m mrad}$.

Halo particle distributions obtained from numerical simulation have the profiles shown in Fig.3 where less than 1 % of the injected particles are halo particles. In order to get statistically meaningful data, large number of halo particles are needed that have similar emittance profiles to those in Fig. 3. Consequently a small program is written to generate the distributions of halo particles to be used for collimator simulation whose emittance profiles are shown in Fig. 4.

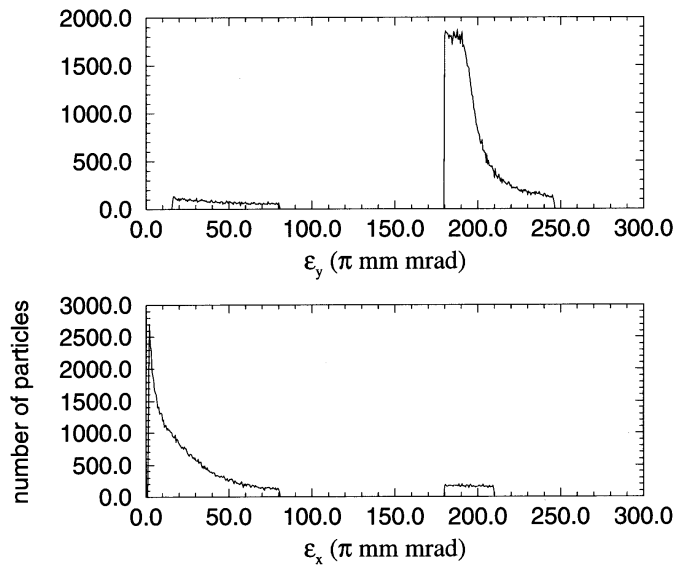


Fig. 4 Plots of emittance profiles of halo particles to be used for the simulations of collimators.

3. Results

- Length of inner collimating tube of collimators

When halo particles hit a collimator face, some of them are scattered back into the collimating tube with large transverse momentum instead of being absorbed by the collimator. These particles are either removed at the later part of the collimating tube or scattered into the collimating tube again (shown in the top plot of Fig. 5). So there are always scattered particles spewed out from the downstream end of a collimator. The vertical line and dots in Fig. 5 at 3.5 m represent these particles where a quadrupole is located. And those particles that have larger transverse displacement than 100 mm at that point might activate the quadrupole to intolerable level. So, it is effective to have as a long inner collimating tube as possible in reducing activation of the following quadrupole and beam pipe. Of course, a longer collimator is more expensive to build. Simulations indicate that at least a 2 m or longer collimating tube is necessary.

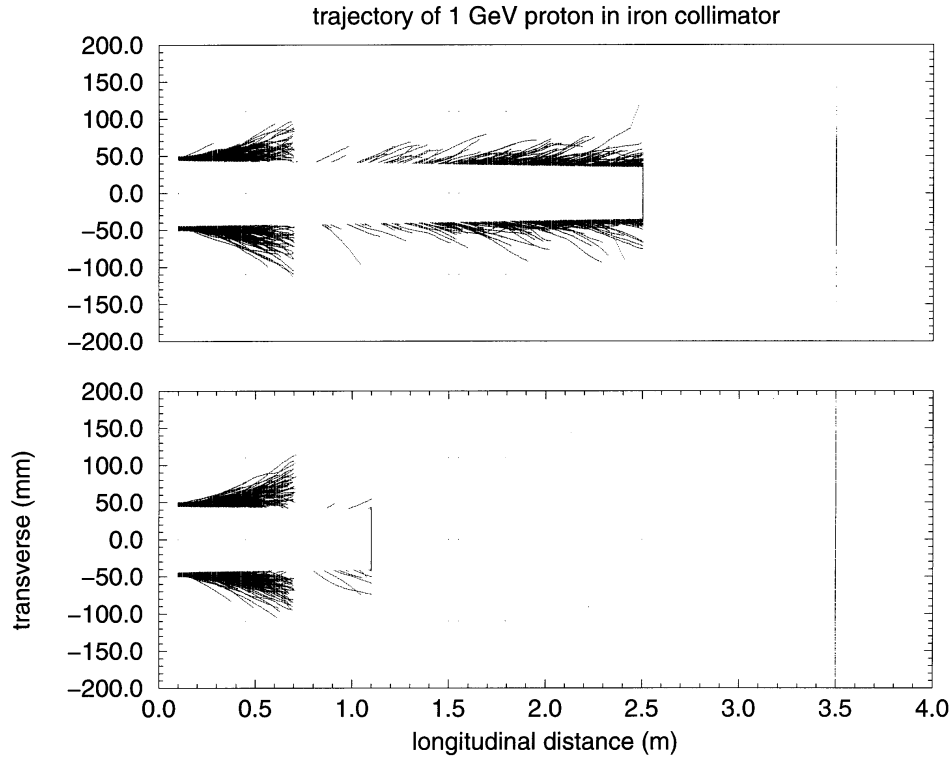


Fig.5 Trajectory of a proton beam inside iron collimators. The collimator in the top plot is 2.4 m long and that in the bottom plot is 1.0 m long. A long collimator is necessary to remove the particles that are scattered into the collimating tube.

- Number and location of collimators

The next question to be answered is the distance between a collimator and the following downstream quadrupole. This distance should be minimized to reduce the activation of the following quadrupole and beam pipe because scattered particles with large transverse momenta reach the beam pipe quickly after a certain drift length. Nevertheless, at least 1 m of space between the collimator and quadrupole should be reserved for maintenance and installation purpose.

The first collimator, that will be called Collimator 1, is a primary collimator both in x and y phase space. A collimator that will be called Collimator 2 should be placed in the next drift space in order to intercept the scattered particles with large transverse momentum from the preceding Collimator 1. Otherwise the scattered particles will activate downstream quadrupoles and beam pipes.

Because the y phase advance between the entrance of Collimator 1 and Collimator 2 is 26 degree, whereas, the corresponding x phase advance is 55 degree, scraping in y phase space by Collimator 2 is less effective than as in x phase space. This is shown in Fig. 6 where the dense line of scattered particles in the top left plot, x-x' phase space, is almost removed in the bottom left plot where another dense line of scattered particles due

to Collimator 2 is observed. On the other hand, there remains appreciable length of the less dense line of scattered particles by Collimator 1 as well as more dense line of scattered particles by Collimator 2 in the bottom right plot, $y-y'$ phase space. Consequently, a third collimator, that will be called Collimator 3, is necessary to scrape effectively in y phase space and to intercept the remaining scattered particles that survive Collimator 1 and 2. Between Collimator 2 and 3, the y phase advance is 55 degree and the x phase advance is 26 degree so that more effective scraping can be done in the y phase space. To reduce further the activation of the down stream components following collimator straight section, a fourth collimator should be placed to remove scattered particles that survive the previous three collimators. In Tables I and II, it is shown that appreciable fraction of scattered particles are absorbed by Collimator 4, which justifies the cost of Collimator 4. Altogether four collimators are necessary to minimize the downstream activation.

Another point worthy of note is that the dense line of scattered particles in the x phase space (left plots) is rather blurred while that in right plots is sharp. This is due to the small residual dispersion in the collimator straight section that is less than 0.3 m.

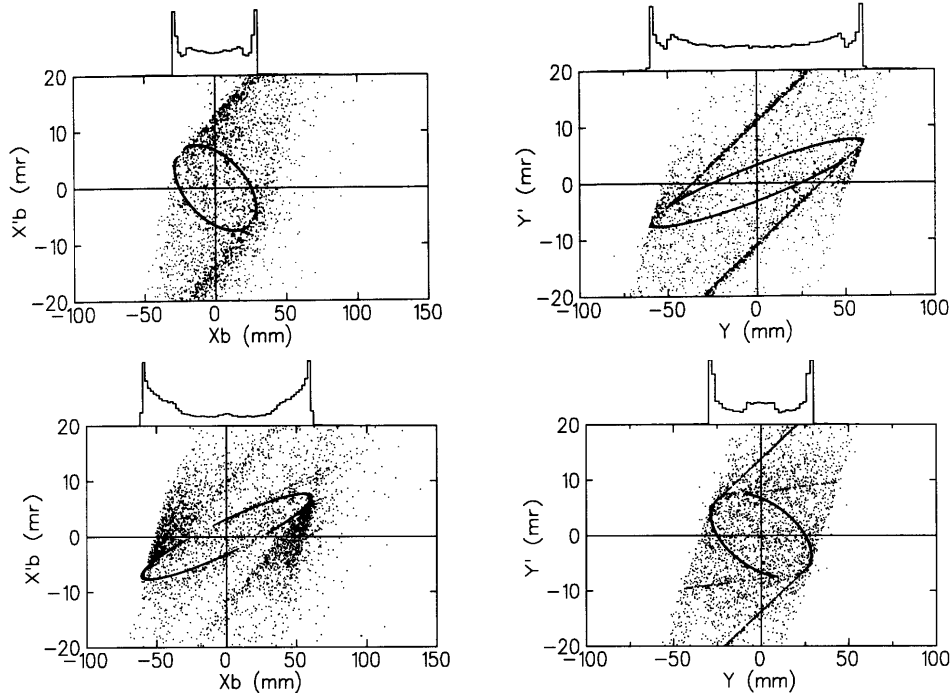


Fig.6 Phase space plots in the x and y planes after collimation. Top (bottom) plot shows particle distributions after passing through the first (second) collimator called Collimator 1 (2).

- Aperture size of secondary collimators

We compare two cases depending on whether Collimator 2 is a primary collimator or not. The loss fractions listed in Table I are based on the halo particle distribution that has the profile of Fig. 3 where the particles are distributed from 180 (180) to 210 (240) p

mm mrad in the x (y) phase space. In Case 1, both Collimator 1 and 2 are primary collimators placed at 180 p mm mrad both in the x and y phase spaces, while Collimator 3 and 4 are secondary collimators placed at 210 p mm mrad both in the x and y phase space. A schematic drawing showing the aperture sizes of Case 1 is given in Fig. 7. In Case 2, only Collimator 1 is a primary collimator placed at 180 p mm mrad both in the x and y phase spaces, while Collimators 2, 3 and 4 are secondary collimators placed at 210 p mm mrad both in the x and y phase space.

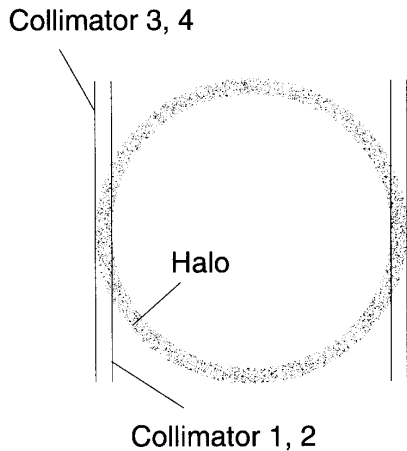


Fig. 7 Aperture sizes of Collimator 1, 2, 3 and 4 of Case 1 of Table I are shown schematically in a normalized phase space where eigenellipses are transformed into circles. All the collimators have rectangular apertures. Collimator 1 and 2 are primary collimators, while Collimator 3 and 4 are secondary collimators.

Table I lists the simulation loss fractions for the two different sets of collimators made of iron. The length of the collimating tubes is 2.4 m and the number of halo particles used in the simulations is 100,000. By taking Collimator 2 as another primary collimator as in Case 1, scraping of halo particles can be done more rapidly (i.e. in less turns) without making the activation of following arc section worse (compare Pipe 6 to 14 of the two cases in Table I). Only changes within statistical errors that are $\pm 0.32 \%$ in activation to the following arc section are observed. Case 1 is also desirable in distributing the activation load more evenly between Collimator 1 and 2. In Case 2, activation load of Collimator 1 is very high, which makes the design of Collimator 1 more difficult. Because Collimator 2 scrapes halo particles as a primary collimator in Case 1, higher activation of the following quadrupole and beam pipe is observed. According to the simulations, noticeable increase of activation of the following beam pipe (Pipe 3 of Table I) is observed compared with the Case 2, while the change in activation of the following quadrupole QF is within statistical error. Pipe 3 probably needs shielding to allow hands on maintenance. Case 1 seems more desirable.

The main function of collimator 3 and 4 is to effectively remove the scattered particles by the previous collimators. In other words, they should be secondary

collimators. The simulation indicates that more than 98 (88) % of halo particles are removed by collimators within 20 (5) turns in Case 1. Consequently, it is reasonable to assume that aperture of Collimator 3 and 4 should be larger than the halo particles generated about in 20 turns. Otherwise, they will act as primary collimators and may produce intolerable amount of scattered particles that will increase activation of the downstream beam line elements.

The aperture of the primary collimators is set to $\sqrt{be_p} - dD$ in order to intercept every particle with the emittance e_p where d is the allowed maximum momentum error and D is the dispersion. On the other hand, the aperture of secondary collimators is set to $\sqrt{be_s}$. Here b is Courant-Snyder parameter and e_p (e_s) is the acceptance of the primary (secondary) collimator.

Table I

	Case 1	Case 2
Collimator 1	57.94 %	89.45 %
QD	0.30 %	0.41 %
Pipe 2	1.40 %	1.78 %
Collimator 2	35.24 %	6.06 %
QF	0.19 %	0.04 %
Pipe 3	1.40 %	0.09 %
Collimator 3	2.71 %	1.41 %
QD	0.01 %	0.01 %
Pipe 4	0.04 %	0.01 %
Collimator 4	0.47 %	0.26 %
QF	0. %	0. %
Pipe 5	0.01 %	0.01 %
Pipe 6	0.02 %	0.01 %
Pipe 7	0.02 %	0.02 %
Pipe 8	0.05 %	0.03 %
Pipe 9	0.01 %	0.01 %
Pipe 10	0. %	0. %
Pipe 11	0.05 %	0.04 %
Pipe 12	0.10 %	0.08 %
Pipe 13	0.01 %	0. %
Pipe 14	0. %	0. %
Sum of Pipe5 to Pipe14	0.27 %	0.20 %

It is worthwhile to point out that due to the maximum dispersion of 4.1 m scattered particles with large momentum deviation, stemming from energy loss due to interactions within collimators, can not survive the downstream arc section, even though they manage to survive four collimators. A momentum collimator may be necessary to intercept these particles instead of having them activate dipoles and quadrupoles in the downstream arc section. For example, see the particle loss at Pipe 11 and 12 listed in Table I and II.

- Activation level of down stream components and material of collimators

Table II lists the cumulative halo particle loss divided by the total number of halo particles at collimators, beam pipes, and quadrupoles as a function of collimator material. The length of the collimators is set to 2.4 m. For the simulations, the halo particles are assumed to have a ± 10 MeV energy spread and assumed to be distributed on the emittance range between 180 and 210 (240) μ m mrad in x (y) phase space. The number of simulated halo particles is 100,000. The distance between a collimator and the following quadrupole is set to 1 m. Collimator 1 and 2 (3 and 4) are primary (secondary) collimators placed at 180 (210) μ m mrad. In determining the horizontal aperture size of the four collimators, the effects of small dispersion in the collimator straight section was also taken into consideration but was negligible. If we assume that 1 % of beam consists of halo to be scraped by the collimators, then the beam loss requirement of 1 nA/m is equal to 0.01 % per meter in Table II.

Table II

	Al ($r=2.70$)	Fe ($r=7.87$)	Cu ($r=8.96$)	W ($r=19.3$)	Pb ($r=11.35$)
Collimator 1	50.71 %	57.94 %	58.44 %	62.37 %	59.97 %
QD	0.34 %	0.30 %	0.35 %	0.28 %	0.56 %
Pipe 2	1.64 %	1.40 %	1.44 %	1.18 %	1.67 %
Collimator 2	35.09 %	35.24 %	35.23 %	34.47 %	34.95 %
QF	0.28 %	0.19 %	0.18 %	0.12 %	0.27 %
Pipe 3	2.30 %	1.40 %	1.28 %	0.49 %	0.90 %
Collimator 3	7.11 %	2.71 %	2.39 %	0.84 %	1.32 %
QD	0.03 %	0.01 %	0.02 %	0.01 %	0.01 %
Pipe 4	0.09 %	0.04 %	0.03 %	0.01 %	0.03 %
Collimator 4	1.44 %	0.47 %	0.37 %	0.13 %	0.21 %
QF	0.02 %	0. %	0. %	0. %	0. %
Pipe 5	0.04 %	0.01 %	0.01 %	0. %	0.01 %
Pipe 6	0.05 %	0.02 %	0.02 %	0. %	0.01 %
Pipe 7	0.06 %	0.02 %	0.02 %	0.01 %	0.01 %
Pipe 8	0.18 %	0.05 %	0.05 %	0.02 %	0.02 %
Pipe 9	0.03 %	0.01 %	0. %	0. %	0. %
Pipe 10	0.01 %	0. %	0. %	0. %	0. %
Pipe 11	0.23 %	0.05 %	0.04 %	0.01 %	0.02 %
Pipe 12	0.28 %	0.10 %	0.09 %	0.03 %	0.03 %
Pipe 13	0.02 %	0.01 %	0.01 %	0.01 %	0. %
Pipe 14	0.01 %	0. %	0. %	0. %	0. %
Sum of Pipe5 to Pipe 14	0.91 %	0.27 %	0.24 %	0.08 %	0.10 %

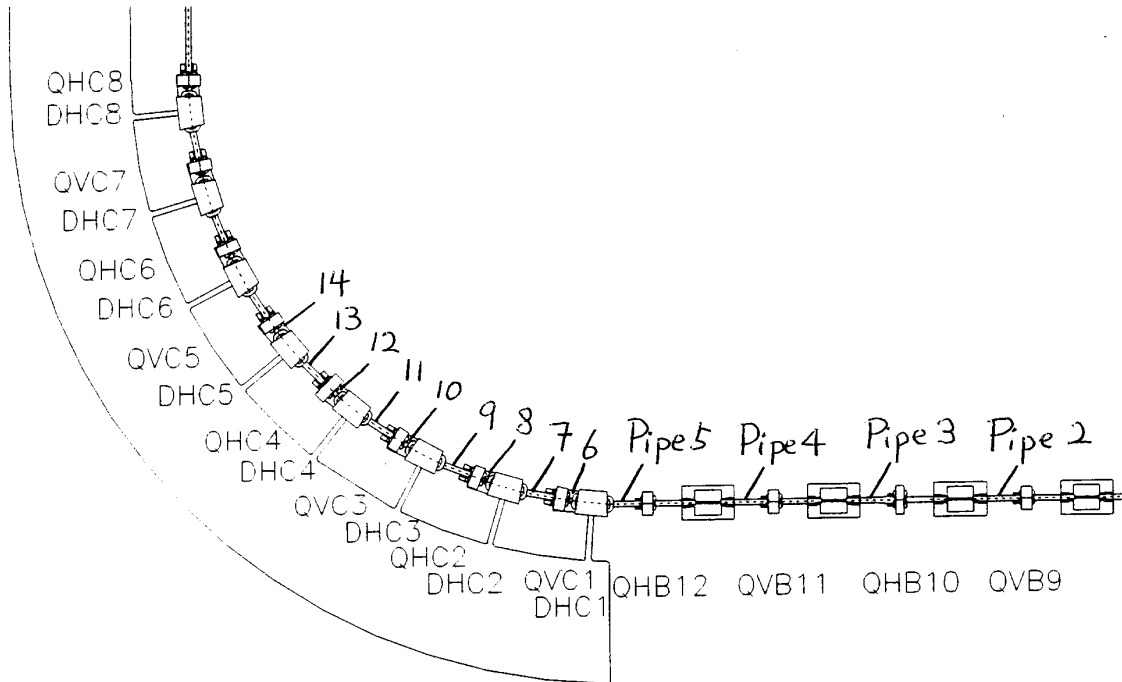


Fig. 8 Plot of the collimator straight section and the downstream arc section with the notation used in Table II. From right to left are Collimators 1, 2, 3 and 4.

Table II shows that the more dense the collimator material is, the less activation downstream components get and the more halo particles are absorbed by primary collimators. Tungsten (W) proves the most effective but it is fairly expensive. It may be considered as an option to install a reasonably thick tungsten collimating tube encompassed by iron. Lead also is effective in this sense. However it produces more neutrons. Overall, iron or copper looks attractive as a compromise material for collimators.

- Observation

About 58 % of halo particles are absorbed by Collimator 1 and about 35 % are absorbed by Collimator 2 for the given halo particle distribution when the collimators are made of iron. On the other hand, only 2.7 % (0.4 %) are absorbed by Collimator 3 (4). Consequently, Collimators 3 and 4 should be designed in a different way from Collimators 1 and 2 according to the much less activation load on them. Because about 1.5 % (1.4 %) are absorbed by the beam pipe “Pipe 2” (“Pipe 3”), definitely movable shielding should be used for them to contain activation and to allow hands on maintenance. And one may make Collimators 3 and 4 as long as possible leaving only minimum space on both sides for installation so that more fraction of scattered particles might be absorbed by secondary collimators rather than by beam pipes.

Rather high beam loss at Pipe 11 and Pipe 12 is due to the fact that dispersion reaches maximum of 4.1 m around Pipe 12 and Pipe 13. It might be necessary to install a

momentum collimator at Pipe 11 to intercept these particles with relatively large energy loss as a result of various interactions with the collimators.

4. Conclusion

Various beam dynamics questions related with the collimators of SNS accumulator ring have been studied. Various factors are optimized with the given ring lattice such as collimating tube length, location, number of collimators, how to set aperture size of primary collimators and secondary collimators, and collimator material. As a result of the beam dynamics study, we learn that movable shielding is necessary for a few hot places that are mostly downstream beam line elements following primary collimators and also that secondary collimators could be designed according to their significantly less activation than that of . Concerning the aperture size of collimators, primary collimators. These simulations indicate that with proper collimation the uncontrolled beam loss requirements of the SNS accumulator ring may be achievable.